Available online at www.sciencedirect.com
ScienceDirect
Solid State Communications 141 (2007) 510–513
solid state communications
www.elsevier.com/locate/ssc

Density and well width dependences of the effective mass of two-dimensional holes in (100) GaAs quantum wells measured using cyclotron resonance at microwave frequencies

H. Zhu[a], K. Lai[b,*,1], D.C. Tsui[b], S.P. Bayrakci[a], N.P. Ong[a], M. Manfra[c], L. Pfeiffer[c], K. West[c]

[a] *Department of Physics, Princeton University, Princeton, NJ 08544, USA*
[b] *Department of Electrical Engineering, Princeton University, Princeton, NJ 08544, USA*
[c] *Bell Labs, Lucent Technologies, Murray Hill, NJ 07974, USA*

Received 30 November 2006; accepted 5 December 2006 by A. Pinczuk
Available online 19 December 2006

Abstract

Cyclotron resonance at microwave frequencies is used to measure the band mass (m_b) of the two-dimensional holes (2DHs) in carbon-doped (100) GaAs/$Al_xGa_{1-x}As$ heterostructures. The measured m_b shows strong dependences on both the 2DH density (p) and the GaAs quantum well width (W). For a fixed W, in the density range (0.4×10^{11} to 1.1×10^{11} cm^{-2}) studied here, m_b increases with p, consistently with previous studies of the 2DHs on the (311)A surface. For a fixed $p = 1.1 \times 10^{11}$ cm^{-2}, m_b increases from $0.22m_e$ at $W = 10$ nm to $0.50m_e$ at $W = 30$ nm, and saturates around $0.51m_e$ for $W > 30$ nm.

PACS: 71.20.Nr; 73.20.Dx

Keywords: A. Semiconductors; D. Cyclotron resonance

For a two-dimensional (2D) system confined in GaAs/$Al_xGa_{1-x}As$ heterostructures, the structure of the valence band is considerably more complicated than that of the conduction band, where a constant electron effective mass well captures the band structure. Due to the 2D quantum confinement, the heavy hole sub-band admixes with the light hole sub-band, giving rise to a highly non-parabolic valence sub-band structure [1–3]. As a result, the hole effective mass (m_b) is a function of many sample-dependent parameters, including the confining potential (the barrier height, the quantum well width, and the doping configuration, etc.), the 2D hole density (p), and the Miller index of the grown surface. Obtaining a full theoretical description of the band structure of the 2D holes is thus a tedious and formidable task [4]. On the other hand, m_b for a GaAs 2D hole system (2DHS) is a very important sample parameter in the research into device application, quantum transport, and optical study, and there have been a number of experimental investigations addressing this issue. However, the earlier cyclotron resonance (CR) experiments were carried out in the high density limit with $p > 1 \times 10^{11}$ cm^{-2} at far infrared frequencies, probing large Landau level separations in the meV energy range (Refs. [5–7]). Only recently have advances in heterostructure crystal growth technology made it possible to materialize 2DHS with density $p \leq 1 \times 10^{11}$ cm^{-2} and mobility sufficiently high to allow low excitation energy microwave CR in the GHz frequency range (Refs. [8,9]).

In physics research of the 2DHS, where high mobility is essential, much work has been done on the silicon-doped samples grown on (311)A GaAs substrates [10]. While the mobility achieved in these 2DHSs is quite impressive, several limitations related to the (311)A surface have been recognized, e.g., the reduced symmetry and the surface corrugation [11]. Recent progress in two kinds of (100)-oriented GaAs 2DHSs effectively removes these constraints. First, the p-type heterojunction insulated-gate field-effect

* Corresponding author.
E-mail address: hanzhu@princeton.edu (H. Zhu).
[1] Present address: Department of Applied Physics, Stanford University, Stanford, CA 94305, USA.

0038-1098/$ - see front matter © 2007 Elsevier Ltd. All rights reserved.
doi:10.1016/j.ssc.2006.12.006

Table 1
Sample parameters, including the Al mole fraction x, the quantum well width W, the 2DH density p, the mobility μ at 0.3 K, and the measured cyclotron mass m_b

Sample	x (%)	W (nm)	p (10^{11} cm^{-2})	μ (10^5 cm^2/V s)	m_b (m_e)
1(8-29-03.2)	32	10	1.1	5.9	0.22
2(9-8-03.1)	32	15	1.1	10.0	0.33
3(1-11-05.1)	16	20	1.1	20	0.54
4(9-8-03.2)	32	30	1.1	7.3	0.50
5(8-21-03.3)	32	Single interface	1.1	5.2	0.51
6(10-30-03.2)	32	50	0.9	5.7	0.48
7(11-17-04.2)	16	10	0.44	8	0.21
8(12-24-03.2)	16	15	0.36	6.6	0.24
9(12-24-03.1)	16	30	0.36	6.6	0.48
10(12-16-04.1)	16	20	0.56	22	0.39

transistors (HIGFETs) on (100) GaAs substrates are now routinely fabricated to study the 2D metal–insulator transition (MIT) [12,13]. Second, instead of silicon, carbon is now used for modulation doping in molecular-beam epitaxy (MBE) growth to produce (100) holes with mobility over 10^6 cm^{-2}/V s [14]. In both cases, the m_b of the (100) 2DHS is needed for probing into the 2D physics. In particular, the strength of the hole–hole interaction is determined by the ratio of the Coulomb energy to the Fermi energy, with the latter inversely proportional to m_b.

In this letter, we report experimental results on m_b, obtained using the cyclotron resonance (CR) technique, for 2DHSs confined in (100) carbon-doped GaAs/Al_xGa_{1-x}As heterostructures. The measured m_b shows strong dependences on both the 2DH density (p) and the GaAs quantum well width (W). For a fixed W, m_b increases with p in the range from 0.36×10^{11} to 1.1×10^{11} cm^{-2}, consistently with previous studies on the (311)A 2DHSs. For a fixed $p = 1.1 \times 10^{11}$ cm^{-2}, m_b increases from $0.22m_e$ at $W = 10$ nm to $0.50m_e$ at $W = 30$ nm, and saturates around $0.51m_e$ for $W > 30$ nm.

We have investigated a total of ten samples in this study, all carbon-doped (100) GaAs/Al_xGa_{1-x}As heterostructures grown by MBE. Except for sample 3, the (asymmetric) δ-doping is from the front only. Important parameters of the individual samples are listed in Table 1, including the Al mole fraction x, the density p, the quantum well width W and the mobility μ measured at 0.3 K, together with the band mass m_b. For most samples, the DC transport data can be found in Ref. [14].

The same cyclotron resonance technique as was previously employed for studying the (311)A p-GaAs samples [10], was used to measure m_b. During a single measurement, the microwave frequency (f) was fixed and the magnetic (B) field was swept. Near the resonance, the 2DHS sample, thinned to 100–150 μm and glued to a sapphire substrate, absorbed the microwave radiation power and its temperature rose above 4.2 K. This temperature difference was detected by an adjacent bolometer glued to the same substrate. In the linear response regime, where our measurements were carried out, the CR amplitude was proportional to the real part of the AC complex conductivity of the 2DHS, which showed a resonance under the condition of $\omega_c = 2\pi f = 2\pi e B_{CR}/m_b$, where B_{CR} was the resonance magnetic field. Further experimental details can be found in Ref. [15].

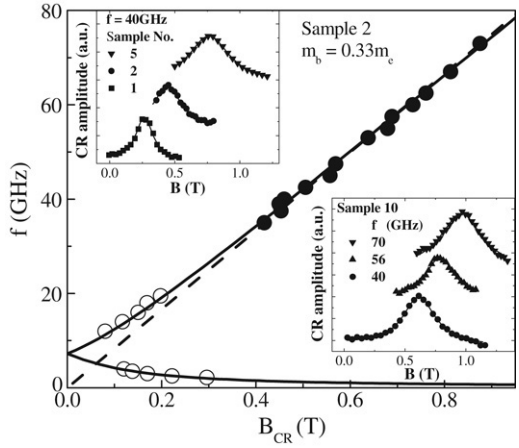

Fig. 1. Microwave frequency f as a function of the resonance magnetic field B_{CR}. The dashed line shows the linear fit to the high f data through zero, which gives a band mass $m_b = 0.33m_e$. The solid line is the fit to all data points (filled and empty circles) using the EMP formula in the text. The inset top left shows the CR signal versus B field for three different samples at $f = 40$ GHz, and the bottom right inset that for sample 10 at three different frequencies.

The two insets in Fig. 1 show the magnetic field dependence of the microwave absorption signal obtained at a fixed frequency of 40 GHz for three different samples, as well as for the same sample at three different frequencies. All curves display a well-defined resonance peak and the line shape of these curves can be fitted by the Drude model [16], shown as the solid lines. In Fig. 1, f is plotted as a function of the peak magnetic field B_{CR} for sample 2. For $f > 35$ GHz, a linear f versus B_{CR} (dashed line) is observed and a mass of $0.33m_e$ is deduced from the slope. For $f < 20$ GHz, however, the data deviate from the linear dependence and the resonance splits into two branches. This behavior is due to coupling of the edge magnetoplasmon (EMP) mode to the cyclotron resonance mode [17]. When this coupling occurs near the EMP frequency ω_0 at $B = 0$ T, the resonant frequency is modified to $\omega_\pm = \pm\omega_c/2 + [(\omega_c/2)^2 + \omega_0^2]^{1/2}$. The thick solid lines in Fig. 1 show the fits to both the low frequency and high frequency parts. The result, $m_b = 0.33m_e$, agrees with that from the linear fit for high frequencies. Fitting to the Drude model and the EMP mode has been discussed in our previous paper [9] and will not be repeated here.

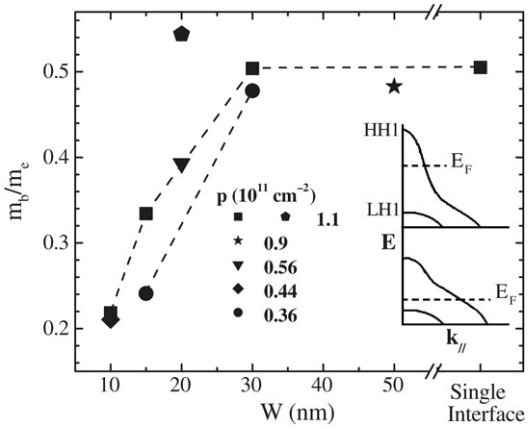

Fig. 2. m_b as a function of W at various 2DH densities in this study (the single-interface sample has $W = 1000$ nm). The dashed lines are guides to the eyes. The two schematics show the possible valence band structures for (upper) narrow quantum wells and (lower) wide quantum wells. E_F in both schematics shows the position of the Fermi level.

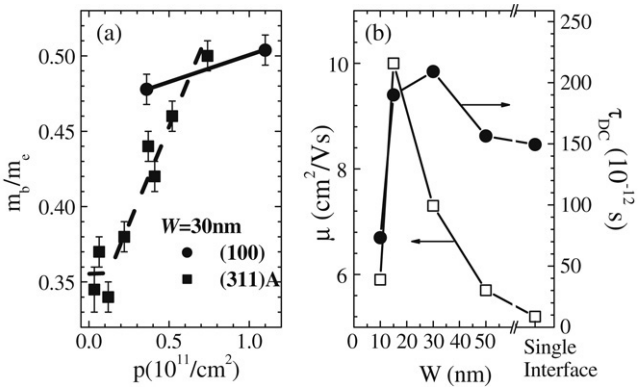

Fig. 3. (a) Comparison of m_b versus p between samples grown on (100) and (311)A substrates. The well width is the same, 30 nm, for the two cases. The lines are guides to the eyes. (b) Transport relaxation time τ_{DC} and mobility μ versus the well width W at $p \sim 1 \times 10^{11}$ cm^{-2} (the single-interface sample has $W = 1000$ nm). The mobility data were taken at $T = 0.3$ K.

Fig. 2 summarizes the results for m_b for our samples. The dependences of m_b on both W and p are readily seen from the plot. For fixed W's at 10 nm, 15 nm, or 30 nm, in the density range (0.36×10^{11} to 1.1×10^{11} cm^{-2}) studied here, m_b increases with p, consistently with previous studies on the 2DHSs on the (311)A surface [9]. For a fixed $p = 1.1 \times 10^{11}$ cm^{-2}, m_b for the four single-side-doped samples (samples 1, 2, 4, and 5) increases monotonically as a function of W and saturates at $0.51m_e$ for $W > 30$ nm, while a larger mass $m_b = 0.54m_e$ is obtained for the symmetrically doped sample (sample 3 with $W = 20$ nm). Our data clearly manifest the complicated valence band structure in (100) GaAs quantum wells.

The density and well width dependences of m_b can be qualitatively understood from the non-parabolic nature of the 2D valence bands [1]. In a quantum well, the fourfold degeneracy of the $J = 3/2$ valence band at the center of the Brillouin zone is removed and the lowest energy hole sub-band is the $J_z = \pm 3/2$ heavy hole sub-band (HH1), which has a small in-plane effective mass. The energy gap separating it from the $J_z = \pm 1/2$ light hole sub-band (LH1) depends strongly on the quantum confinement. Away from the zone center, the HH and LH bands mix giving rise to level anticrossing and highly non-parabolic, anisotropic in-plane dispersion. At a fixed W, the non-parabolic effect is small when the density is low and the Fermi contour is nearly a circle. The m_b is heavier at higher densities because the non-parabolic effect becomes important. In fact, it has been shown that the Fermi contour here is significantly distorted [18]. For samples with different W's, the confinement is stronger in smaller W samples, giving rise to a larger band splitting. As illustrated in the insets of Fig. 2, for narrow well samples with $W = 10$ nm, the splitting is so large that the measured $m_b = 0.21m_e$ for $p = 0.44 \times 10^{11}$ cm^{-2} and $0.22m_e$ for $p = 1.1 \times 10^{11}$ cm^{-2}, practically independent of p. In fact, in our previous experiments in (311)A 2DHSs, a mass of $0.19m_e$ is also observed for the 10 nm narrow well sample [10]. For wide wells with $W > 30$ nm, on the other hand, the splitting at the zone center is small. As a result, even in our low density sample with $p = 0.36 \times 10^{11}$ cm^{-2}, the Fermi level E_F may already be at an energy sufficiently away from the HH1 and LH1 level anticrossing that m_b depends only weakly on p. Interestingly, it is suggestive from our limited data points that for $W = 15$–20 nm, the strong density dependence of m_b is due to the sub-band non-parabolicity in the level anticrossing region of the in-plane dispersion. Experiments are under way to measure m_b for various p's at a fixed $W = 20$ nm. We nevertheless want to emphasize that the real band structure of the 2DHS has a much more complicated shape and our oversimplified picture can explain the data only qualitatively.

Finally, two remarks on the data are in order. First, in Fig. 3(a) we compare the m_b versus p relation for the (311)A [10] and the (100) p-GaAs 2DHSs at the same quantum well width $W = 30$ nm. It appears that the density dependence of m_b is weaker for the 2DHS in the (100) orientation than for that in (311)A. Second, our data help to shed some light on the puzzling transport data previously reported by Manfra et al. [15]. In Fig. 3(b), we plot the transport mobility (μ) measured at $T = 0.3$ K and the DC relaxation time ($\tau_{DC} = \mu m_b/e$) as a function of the well width W at $p \sim 1 \times 10^{11}$ cm^{-2}. It is clearly seen that μ for these samples shows a sharp peak at $W = 15$ nm, which is in contrast to the case for the GaAs 2D electron system with monotonically increasing μ versus W. It was conjectured that this anomalously high μ at $W = 15$ nm may not be due to a large τ_{DC}, but instead the change of other material parameters like m_b. Indeed, we observe in Fig. 3(b) that, because of the m_b at $W = 15$ nm being smaller than that at 30 nm, τ_{DC} is actually shorter at $W = 15$ nm. However, even after taking into account the effect of m_b, $\tau_{DC} = 0.21$ ns at $W = 30$ nm is still longer than that for wider wells.

To summarize, we have experimentally determined the band mass of 2DHSs in carbon-doped p-type (100) GaAs/$Al_xGa_{1-x}As$ heterostructures. The measured m_b shows strong dependences on both the 2D hole density p and the well width W. The fact that m_b increases with either p or W is qualitatively consistent with the nature of non-parabolic 2D valence bands.

Acknowledgements

The authors would like to thank Wei Pan, Minhyea Lee, and Lu Li for helpful discussions and experimental assistance. The work at Princeton was supported by the NSF. S.P.B. and N.P.O. acknowledge support from NSF MRSEC grant DMR 0213706.

References

[1] D.A. Broido, L.J. Sham, Phys. Rev. B 31 (1985) 888.
[2] U. Ekenberg, M. Altarelli, Phys. Rev. B 32 (1985) 3712.
[3] G. Goldoni, F.M. Peeters, Phys. Rev. B 51 (1995) 17806.
[4] See, for example, Table II in P. Pfeffer, W. Zawadzki, Phys. Rev. B 53 (1996) 12813.
[5] H.L. Stormer, Z. Schlesinger, A. Chang, D.C. Tsui, A.C. Gossard, W. Wiegmann, Phys. Rev. Lett. 51 (1983) 126.
[6] Z. Schlesinger, S.J. Allen, Y. Yafet, A.C. Gossard, W. Wiegmann, Phys. Rev. B 32 (1985) 5231.
[7] K. Hirakawa, Y. Zhao, M.B. Santos, M. Shayegan, D.C. Tsui, Phys. Rev. B 47 (1993) 4076.
[8] B.E. Cole, J.M. Chamberlain, M. Henini, T. Cheng, W. Batty, A. Wittlin, J.A.A.J. Perenboom, A. Ardavan, A. Polisski, J. Singleton, Phys. Rev. B 55 (1997) 2503.
[9] W. Pan, K. Lai, S.P. Bayrakci, N.P. Ong, D.C. Tsui, L.N. Pfeiffer, K.W. West, Appl. Phys. Lett. 83 (2003) 3519.
[10] M.B. Santos, Y.W. Suen, M. Shayegan, Y.P. Li, L.W. Engel, D.C. Tsui, Phys. Rev. Lett. 68 (1992) 1188.
[11] J.J. Heremans, M.B. Santos, K. Hirakawa, M. Shayegan, J. Appl. Phys. 76 (1994) 1980.
[12] B.E. Kane, L.N. Pfeiffer, K.W. West, C.K. Harnett, Appl. Phys. Lett. 63 (1993) 2132.
[13] H. Noh, M.P. Lilly, D.C. Tsui, J.A. Simmons, L.N. Pfeiffer, K.W. West, Phys. Rev. B 68 (2003) 241308;
J. Huang, D.S. Novikov, D.C. Tsui, L.N. Pfeiffer, K.W. West, 2006 cond-mat/0603053.
[14] M.J. Manfra, L.N. Pfeiffer, K.W. West, R. de Picciotto, K.W. Baldwin, Appl. Phys. Lett. 86 (2005) 162106.
[15] Y. Matsuda, N.P. Ong, Y.F. Yan, J.M. Harris, J.B. Peterson, Phys. Rev. B 49 (1994) 4380;
S.P. Bayrakci, Ph.D. Thesis, Princeton University, 1999.
[16] G. Dresselhaus, A.F. Kip, C. Kittel, Phys. Rev. 98 (1955) 368.
[17] S.J. Allen, H.L. Stormer, J.C.M. Hwang, Phys. Rev. B 28 (1983) 4875.
[18] J.A. Kash, M. Zachau, M.A. Tischler, U. Ekenberg, Phys. Rev. Lett. 69 (1992) 2260.